Desalination and Water Treatment
www.deswater.com

doi: 10.5004/dwt.2018.23114

136 (2018) 320–331
December

Influence of H^+ and Na^+ ions on the morphology of titanate nanomaterial and its adsorption property of lead

Gongduan Fan[a,*], Xiaomei Zheng[a], Huiping Peng[a], Jing Lou[a], Pei Hua[b], Jin Zhang[c,*]

[a]*College of Civil Engineering, Fuzhou University, 350116 Fujian, China, email: fgdfz@fzu.edu.cn (G. Fan), Tel. +86 591 22865361; Fax: +86 591 22865355; emails: n160520053@fzu.edu.cn (X. Zheng), n160527036@fzu.edu.cn (H. Peng), 727919985@qq.com (J. Luo)*
[b]*Institute of Urban Water Management, Technische Universität Dresden, 01062 Dresden, Germany, email: pei.hua@hotmail.com*
[c]*Institute of Groundwater and Earth Sciences, Jinan University, 510632 Guangzhou, China, email: jzhang@jnu.edu.cn*

Received 26 March 2018; Accepted 11 September 2018

ABSTRACT

Ion-exchange induced adsorption behaviors of heavy metals onto the titanate nanomaterials is essential to facilitate their application for removing heavy metals from the aquatic environment. This study evaluates the adsorption mechanisms of Pb(II) on hydrogen (TNs-H) and sodium (TNs-Na) titanate materials synthesized through a facile one-step hydrothermal method followed by washing with acid and water. The physical–chemical properties of the TNs including morphology, structure, surface area and chemical composition were studied, and the adsorption capacity of TNs to Pb(II) was tested. The results showed that TNs were pure monoclinic titanate with plate morphology and specific surface area of ~246 m^2/g. The adsorption capacity of TNs-H was 120 mg/g, while TNs-Na reached 450 mg/g, which indicated that water-washing with large interlayer spacing could increase the adsorption capacity of TNs. The adsorption kinetics followed pseudo-second-order model and the equilibrium data were best fitted with Langmuir isotherm model. After six runs of reuse, the adsorption capacity basically remains the same. Results presented here would facilitate titanate nanomaterials' application to remove heavy metals from aquatic environment.

Keywords: Titanate nanomaterials; Synthesis washing specimen; Adsorption isotherm; Adsorption kinetics; Lead

1. Introduction

Industrial effluents, which are loaded with heavy metals even at trace level, are believed to be a risk for humans and have a severe environmental impact. Unlike organic wastes, heavy metals are non-biodegradable, and they can be accumulated in living tissues, causing various diseases and disorders [1]. For this reason, the maximum allowable limit of their discharge is more and more stringent, and they must be removed before discharged. Lead is a relatively unreactive post-transition metal. It is usually used as an industrial raw material for rechargeable battery, printing, pigments, fuels, photographic processing and secondary explosives [2–4]. The lead pollution threatens the health of human beings by ways of the drinking water and food chain. Pb(II) is non-essential to human body but excessive intake may damage the brain, nervous and immune system [3].

There are several methods for removing heavy metal from aquatic environments, for example, chemical precipitation [5,6], ion exchange [7], membrane filtration [8], electrochemistry process [9] and adsorption technologies. Compared with other techniques, adsorption is a highly efficient, economy and eco-friendly technology for eliminating heavy metals at relatively low concentration and it reliably generates high-quality effluent [4,10,11]. Moreover, it is flexible in design and operation as the adsorption process is reversible which facilitates the adsorbent regeneration and the toxic sludge treatment [12,13]. Due to its high efficiency and flexibility, the adsorption process has become a promising technique in industrial application.

* Corresponding authors.

Nowadays, there are a variety of traditional and modern adsorbents, such as clay minerals, nanosized metal oxides, layered double hydroxides, carbonaceous materials, metal-organic frameworks and so on [14]. Among the adsorbents, titanate nanomaterials (TNs) are nanomaterials which first applied on 1990's. These materials have been widely adopted in the adsorption field due to a variety of advantages such as unique physicochemical features, excellent ion exchange capacities, large specific surface areas and low secondary pollution impact on the environment [15,16]. Furthermore, TNs synthesized using hydro-thermal method under different reaction conditions or subsequent modification methods will significantly affect the morphology and physicochemical properties of the final product [17]. Literatures are available on the role of ion-exchange between sodium (Na^+) and proton (H^+) on the morphology of TNs in the research matrix of photocatalytic activity [18], electrochemical lithium storage [19], etc. However, there has been less systematic examination of the ion-exchange induced adsorption behaviors of heavy metals onto the TNs.

In addition, it is well-known that adsorption efficiency depends on various experimental factors, such as adsorbent dosage, initial adsorbate concentration, temperature and solution pH value [20–23]. Therefore, an in-depth physical and chemical study on the adsorptive properties of sodium and hydrogen titanate is essential to facilitate their application for removing heavy metals from the aquatic environment.

Consequently, the primary focus of this study is to evaluate the adsorption mechanisms of Pb(II) on hydrogen and sodium titanate materials synthesized through a facile one-step hydrothermal method followed by washing with acid and water. The morphology and crystal phase of the titanate materials were characterized. The effects of various operational conditions such as contact time, pH and adsorbent dosage were systematically studied. The adsorption kinetics and isotherms were also analyzed to reveal the adsorption mechanisms. The data presented here could be of importance for titanate materials synthesis and its use for environmental remediation.

2. Materials and methods

2.1. Chemical reagents

TiO_2 (titanium dioxide, 80% anatase and 20% rutile) powders, NaOH (sodium dydroxide), HCl (hydrochloric acid), $Pb(NO_3)_2$ (lead nitrate) were purchased from Sinopharm Chemical Reagent Co. Ltd. All the chemicals used in this study were of analytical grade except $Pb(NO_3)_2$. $Pb(NO_3)_2$ was of guarantee reagent. $Pb(NO_3)_2$ was used to prepare the Pb(II) stock solution (1,000 mg/L).

2.2. Synthesis of titanate nanomaterials

The TNs were synthesized under the hydrothermal conditions reported by Wei et al [24]. Briefly, 1.0 g of commercial TiO_2 nanoparticle powder (P25) and the aqueous solutions of NaOH (10 M, 100 mL) were deposited into a Teflon container. The mixture was vigorously stirred in an oil bath at 110°C for 72 h and then was cooled to room temperature. The milk-like suspension was filtrated. Hydrochloric acid (HCl, 10 M) and deionized water were selected as the washing specimen to form TNs-H ($H_2Ti_3O_7$) and TNs-Na ($Na_2Ti_3O_7$), respectively. The washing process was stopped until the pH value approaching 7 ± 0.1. Finally, the white products were dried in an oven at 70°C for 8 h. The dry samples were then ground, concentrated, labeled and stored in the glass bottles until analyzed. The prepared samples and the samples which Pb(II) adsorbed on were characterized.

2.3. Characterization of titanate nanomaterials

The prepared samples and the samples which Pb(II) adsorbed on were ground. The composition of these samples was analyzed by XRD (X'Pert PRO X-ray powder diffraction, PANalytical Co. Ltd., Holland) using Cu Kα radiation (λ = 1.5418 Å), which later switched to Cu Kα radiation, with a scanning range of 5°C–75°C. The morphologies of TNs were investigated by a FE-SEM (S4800, Hitachi Co. Ltd., Japan) and a TEM (HRTEM, TECNAL G2F20, FEI Co. Ltd., USA), respectively. The pore volume, BET surface area and pore size of materials were analyzed at 77 K (–296.15°C) and the samples were degassed at 423 K (49.85°C) for 6 h. The pore size distributions of TNs were calculated by the method of Barrett–Joyner–Halenda (BJH). The infrared spectra of samples were measured by FT-IR (FT-IR, Nicolet 6700, Thermo Fisher Scientific Co. Ltd., USA), which needed to be previously prepared by the KBr pellet pressing method with a measurement range and distinguishability of 4,000–400 cm^{-1} and 4 cm^{-1}, respectively.

2.4. Adsorption experiment

The adsorption behaviors of Pb(II) from aqueous solutions onto TNs were investigated by batch adsorption experiments. Briefly, a specific dosage of TNs was added into a specified volume of solution containing a certain concentration of Pb(II). The mixture in the conical flask (200 mL) was shaken in a rotary shaker at 200 rpm. At the designed adsorbing time, about 5 mL solution was centrifuged at a speed of 5,000 rpm for 5 min to obtain the supernatant. The supernatant was filtered through 0.45 μm membrane and diluted to desired volumes. Pb(II) concentration was determined using an inductively coupled plasma optical emission spectrometry (ICP-OES Optima 7000, PerkinElmer, USA). More details are as follows:

To investigate the adsorption properties of TNs for Pb(II) in aqueous solutions, the following parameters were considered, that is, adsorption time, initial heavy metal concentrations, pH values and adsorbent dosages. The detailed adsorption scenarios were described as follows:

1. Effect of adsorption time: The initial concentrations of Pb(II) and TNs were 200 mg/L and 1.0 g/L, respectively. The sampling time was 0, 1, 3, 5, 7, 10, 20, 40, 60, 80, 120, 180 and 240 min at the temperature of about 20°C ± 0.1°C.
2. Effect of initial heavy metal concentration: The pH value was about 5.2 ± 0.1. The dosage of TNs was 0.2 g/L. The oscillating time was 6 h to ensure the adsorption time according to the previous adsorption equilibrium experiment. The initial heavy metal concentrations were 5, 10, 20, 50, 100, 200, 300 and 400 mg/L.

3. Effect of pH: The initial concentration of Pb(II) and TNs were 300 mg/L and 1.0 g/L, respectively. The oscillating time was 6 h. The initial pH values of Pb(II) solution were adjusted to 1.0, 2.0, 3.0, 4.0, 5.0 and 6.0 individually by using dilute HCl and NaOH (0.1 M) at the temperature of about 20°C ± 0.1°C..
4. Effect of adsorbent dosage: The initial concentration of Pb(II) was 100 mg/L with the value of 5.2 ± 0.1. The temperature was 20°C ± 0.1°C. The dosages of TNs were 0.05, 0.1, 0.2, 0.4, 0.7, 1.0, 1.5 and 2.0 g/L, respectively.
5. Desorption experiment: Hydrochloric acid was used as a desorption agent. The initial concentration of Pb(II) was 100 mg/L. The oscillating time was 6 h under the temperature of 20°C ± 0.1°C. The initial concentration C_0 and equilibrium concentration C_e of heavy metals were investigated after the equilibrium was reached. The pH values of the equilibrium solution were adjusted to 1.0–6.0. After 6 h of continuous stirring to achieve an equilibrium. The desorption equilibrium concentration of heavy metal C_d was then measured.

The amount of metal ion adsorbed q_t at time t (min) was calculated by Eq. (1):

$$q_t = \frac{(C_0 - C_t)V}{m} \tag{1}$$

where C_0 and C_t are metal concentrations at beginning and time t (min), respectively, V (L) is the volume of metal ion solution, and m (g) is the dry mass of the titanate nanomaterials.

The amount of metal adsorbed at equilibrium q_e (mg/g), the metal ion removal efficiency R (%) and the desorption efficiency D (%) were calculated by Eqs. (2)–(4), respectively.

$$q_e = \frac{(C_0 - C_e)V}{m} \tag{2}$$

$$R = \frac{C_0 - C_e}{C_0} \times 100 \tag{3}$$

$$D = \frac{C_0 - C_e}{C_0 - C_d} \times 100 \tag{4}$$

where C_e and C_d (mg/L) are metal equilibrium concentrations of adsorption and desorption, respectively.

2.5. Modeling of the adsorption kinetics

The adsorption kinetics of Pb(II) onto TNs were further investigated. The adsorption datasets of Pb(II) from aqueous solutions whose initial concentration of Pb(II) was 200 mg/L were analyzed and fitted with three kinetic models, that is, pseudo-first-order kinetic, pseudo-second-order kinetic and intraparticle diffusion models (shown in Table 1). Pseudo-first-order proposed at the end of the 19th century [25], and pseudo-second-order mechanisms introduced in the middle of the 80's [26]. If initially no adsorbate presents the adsorbent, then assuming the first-order rate kinetics the fractional uptake on the adsorbate by the adsorbent can be expressed as equation in Table 1. The pseudo-second-order model is based on the assumption of chemisorption of the adsorbent. The kinetic rate model can be represented as equation in Table 1.

2.6. Modeling of adsorption isotherm

The adsorption isotherms provide the distribution proportions of the adsorbate, adsorbent and solution. It can also reflex the adsorption capacity of the adsorbent to adsorbate. Hence, the equilibrium Pb(II) data were further analyzed by three isotherm models with different initial concentrations, that is, Langmuir [27], Freundlich [28] and Temkin isotherm models [29]. More explicit, Langmuir model assumes an even distribution of the adsorption sites on the surface of the adsorbent. The absorption is a monomolecular type. Pollutants adsorbed on the surface of adsorbent are non-interacting in this case [30]. Freundlich isotherm is an empirical equation describing heterogeneous surface adsorption of adsorbent to adsorbate [31], and Temkin [29] model considers the interaction between adsorbates. The models of adsorption isotherm are shown in Table 2.

Table 1
Modeling of the adsorption kinetics

Kinetic model	Formula	Kinetic parameters
Pseudo-first-order kinetic model [11]	$\log(q_e - q_t) = \log q_e - \frac{k_1}{2.303}t$	q_e (mg/g) and q_t (mg/g) are the equilibrium adsorption capacity and adsorption amount at time t, respectively, t (min) is the contact time between the adsorbent and metal ions, k_1 (1/min) is the pseudo-first-order rate constant
Pseudo-second-order kinetic model [12]	$\frac{t}{q_t} = \frac{1}{k_2 q_e^2} + \frac{1}{q_e}$	k_2 (g/(mg·min)) is the pseudo-second-order rate constant
Intraparticle diffusion model [13]	$q_t = k_{\text{int}} t^{0.5} + C$	k_{int} (mg/(g·min$^{0.5}$)) is the rate constant of intraparticle diffusion, and C (mg/g) is the constant proportional to the extent of boundary layer thickness

Table 2
Modeling of adsorption isotherm

Isotherm model	Formula	Kinetic parameters
Langmuir	$\frac{C_e}{q_e}=\frac{1}{bQ}+\frac{1}{Q}C_e$	C_e (mg/L) the equilibrium concentration of metal ion, q_e (mg/g) is the corresponding equilibrium adsorption capacity, Q (mg/g) is the calculated maximum adsorption capacity, b (L/mg) is the Langmuir equation constant standing for free energy of adsorption
Freundlich	$\log q_e=\log K_F-\frac{1}{n}\log C_e$	K_F (mg/g) is the Freundlich constant related to adsorption capacity, and n is an intensity factor reflecting the adsorption intensity of the adsorbent.
Temkin	$q_e=\frac{RT}{B}\ln A-\frac{RT}{B}\ln C_e$	A (L/g) and B (J/mol) are Temkin constants, R (J/mol K) is the ideal gas constant and T (K) is the absolute temperature

2.7. Reuse of TNs-Na and TNs-H

After adsorption process, the nanomaterials were reused in desorption (TNs-des) and regeneration (TNs-re) process. The main recycle process was the adsorption–desorption–regeneration–adsorption. In adsorption, the 400 mL Pb(II) solution with the initial concentration of 150 mg/L and 0.8 g/L TNs were used. In desorption, the pH was adjusted to 1 by 0.1 M HCl. The desorption process was carried out for 5 h. Then, the TNs were centrifuged, dried and weighed, marked as TNs-des. In regeneration, 0.2 M NaOH was used to regenerate for 5 h, and the regenerated TNs were also centrifuged, dried, weighed and marked as TNs-re. After that, both of TNs-des and TNs-re were used to remove the Pb(II) for six cycles.

3. Results and discussion

3.1. Characterization of TNs

3.1.1. XRD analysis

The X-ray diffraction pattern of TNs-H, TNs-Na, TNs-H-Pb (TNs-H adsorbed Pb), and TNs-Na-Pb (TNs-Na adsorbed Pb) are depicted in Fig. 1. It shows that TNs-Na has diffraction peaks at ca. 2θ ≈ 10°, 24°, 28° and 48°. TNs-H has diffraction peaks at ca. 2θ peaks at 24° and 48°. It has been reported that a peak at ca. 2θ ≈ 10° was observed for the interlayer space of TNs [32]. Therefore, the results indicate that those two samples were titanates with pure monoclinic phase and had a good crystallinity. The chemical composition of the synthesized TNs-Na and TNs-H could be described as $Na_2Ti_3O_7$ and $H_2Ti_3O_7$, respectively [33]. Compared with TNs-Na, the intensity of the diffraction peak of TNs-H at 2θ ≈ 10° and 28° decreased and eventually disappeared, which confirmed that the interlayer space and titanate (111) crystal plane would be destroyed by pickling [33].

Furthermore, the diffraction peaks of TNs-H-Pb and TNs-Na-Pb had no considerable changes. It is mainly because the crystal structure of TNs has not changed in the process of adsorption. The results indicate that adsorption of Pb(II) onto TNs occurs mainly when the ion exchange was carried out in the interlayer of TNs. However, the decreased intensity of the diffraction peak of TNs-H-Pb and TNs-Na-Pb at 2θ ≈ 10° indicates that the adsorbed Pb(II) changed the interlayer distance of TNs.

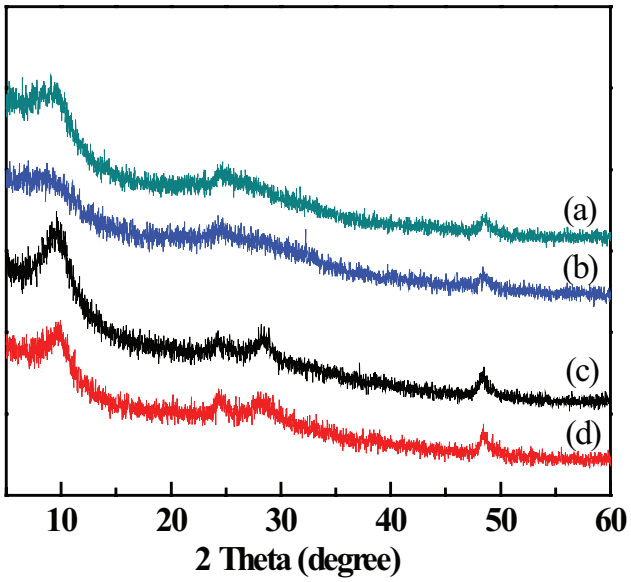

Fig. 1. XRD patterns of (a) TNs-H, (b) TNs-H-Pb, (c) TNs-Na and (d) TNs-Na-Pb.

3.1.2. SEM and TEM analysis

As shown in Figs. 2(a) and (b), TNs synthesized by hydrochloric acid and deionized water washing approaches were nanostructures with flaky morphology and most of the nanosheet was disorderly winded. Compared with TNs-H, to some extent, SEM image of TNs-Na was longer and slender, indicating that the different washing specimen induced different morphology features of TNs were distinctive. According to the TEM image shown in Fig. 2, TNs synthesized by different washing approaches was titanate of plate morphology with glaze surface. There were some similar morphologies between TNs-H and TNs-Na. Each nanosheet of a length is hundreds of nanometers or even exceeded 1 μm and nanosheet of a width is scarcely 200 nm feet. In other words, the synthesized products have a high length–diameter ratio and a good dispersion, which is inconsistent with the previous study [34]. More explicitly, as shown in Figs. 2(d) and (f), the surface of TNs adsorbed Pb(II) became rough. Numbers of "dark dots" appeared, demonstrating that Pb(II) adsorbed on the surface of TNs [35]. Meanwhile, no apparent variation and destruction were observed along the layered

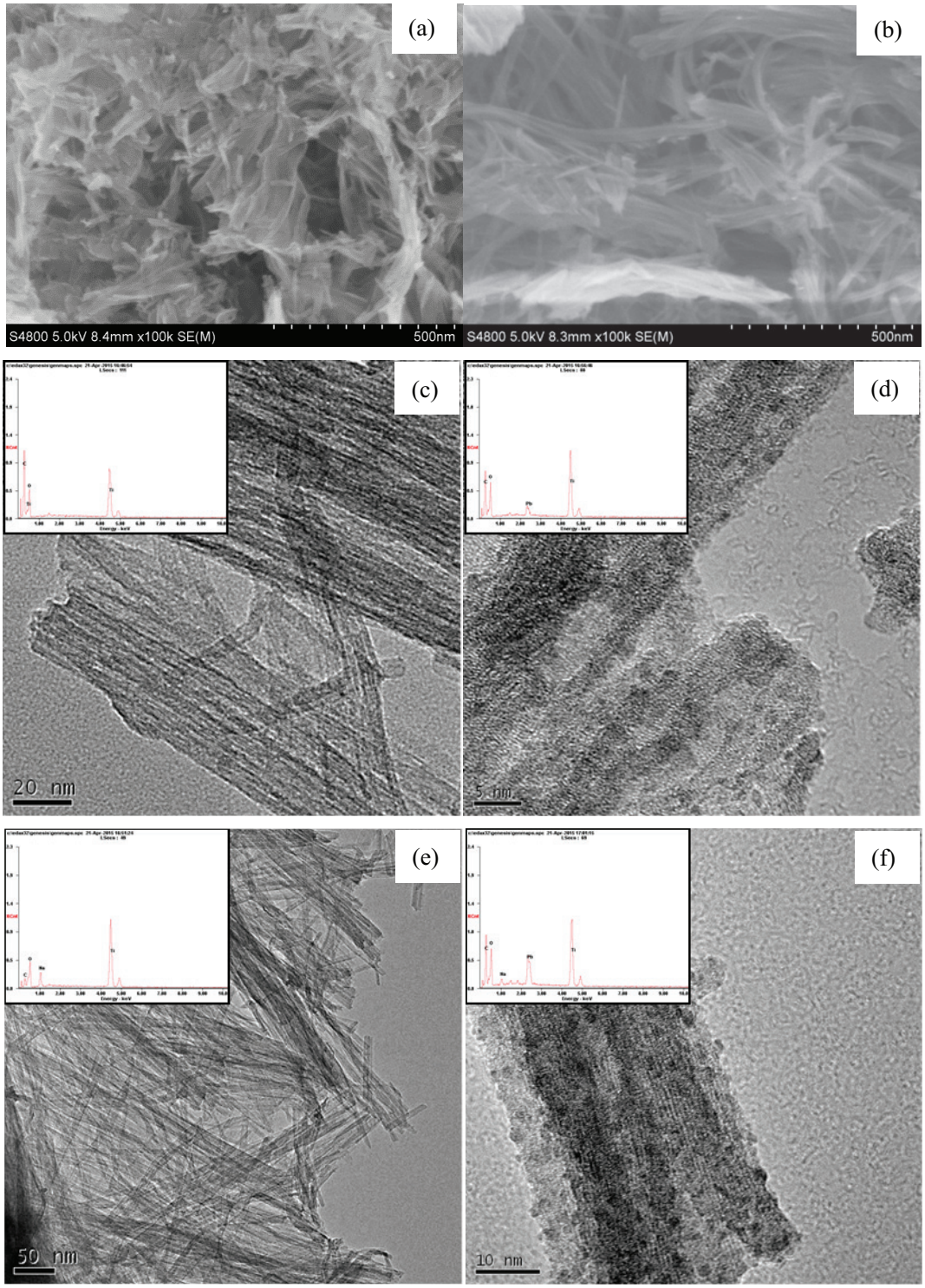

Fig. 2. SEM images of (a) TNs-H and (b) TNs-Na; TEM images of (c) TNs-H, (d) TNs-H-Pb, (e) TNs-Na and (f) TNs-Na-Pb.

structure and sheet-like morphology of TNs, suggesting that the adsorption process only caused minor damage to titanate nanotubes (TNTs) structures. Moreover, as shown in Figs. 2(c) and (e), it is obvious that TNs-H was free from Na^+ ion, while TNs-Na was full of the Na^+ ion. The results indicate that the main difference between TNs-H and TNs-Na would be the main factor that affects the adsorption of Pb(II).

3.1.3. Specific surface area analysis

The adsorption–desorption isothermal and pore size distribution of TNs are shown in Fig. 3. As can be seen, adsorption isotherms for those samples were type Ⅳ with H3 hysteresis loop [36], which indicates the mesoporous structural conditions.

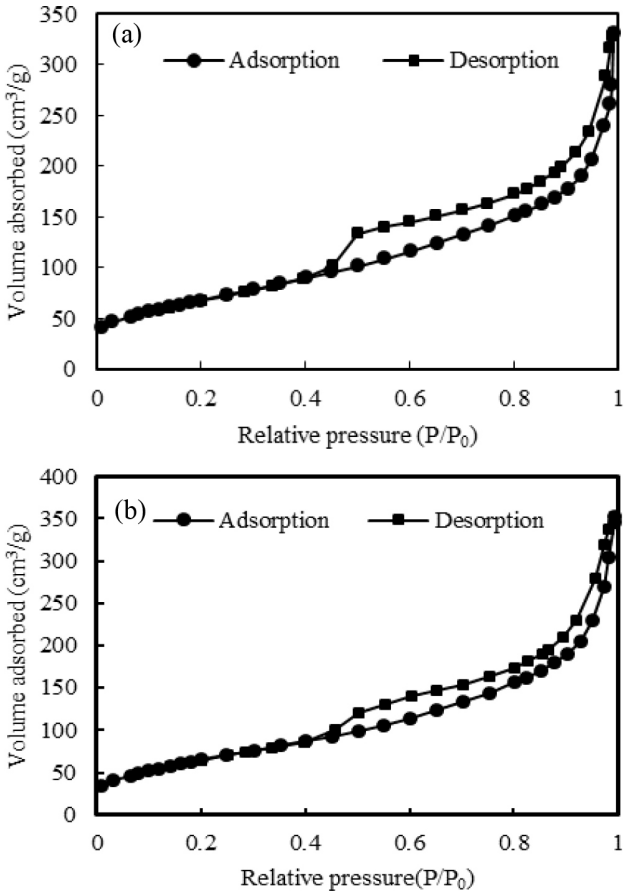

Fig. 3. N_2 adsorption–desorption isotherms of TNs ((a) TNs-H, (b) TNs-Na).

Physical properties of those materials are shown in Table 3. Specific surface area and pore volume of TNs-H were 246.82 m^2/g and 0.551 cm^3/g, respectively, while that of TNs-Na were 246.03 m^2/g and 0.544 cm^3/g, respectively. There is no significant difference in physical properties between TNs-H and TNs-Na, indicating washing ways and kinds of ions carried on the surface have limited effects on physical properties of materials.

3.2. Adsorption of Pb(II) onto TNs

3.2.1. Effect of contact time

The study of adsorption kinetics describes the solute uptake. 200 mg/L Pb(II) initial concentration was applied to investigate the effect of contact time on the adsorption of Pb(II) onto TNs in aqueous solutions after 300 min. As shown in Fig. 4, the adsorption process of Pb(II) can be divided into two steps of a fast phase and a slow phase. First, within the first 20 min, the adsorption rate of Pb(II) was very fast that the TNs-Na reached 7.05 mg/min and the TNs-H reached 3.99 mg/min, respectively, which consisted with the findings of Xiong et al. [34]. Especially, the adsorption rate in the first 5 min was the fastest during the whole process that TNs-Na up to 25.29 mg/min and TNs-H up to 14.83 mg/min, and the adsorption capacities of TNs-H and TNs-Na for Pb(II) reached at 74.14 mg/g and 126.43 mg/g, respectively. Moreover, the

Table 3
Basic structure parameters of TNs

Parameters	TNs-H	TNs-Na
Surface area (m^2/g)	246.82	246.03
Pore volume (cm^3/g)	0.551	0.544

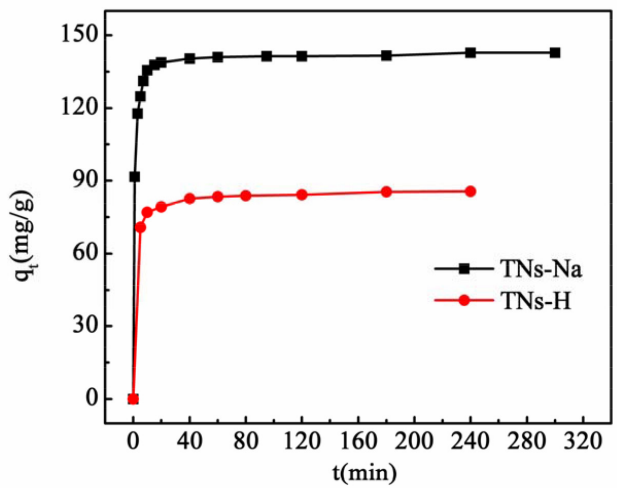

Fig. 4. Effect of contact time on the adsorption of Pb(II) by TNs.

adsorption curves of those samples in the first 5 min almost overlap each other, which indicate that the adsorption tendencies of those two samples were consistent. With the further increase of contact time up to 20 min, the adsorption capacities of TNs-H and TNs-Na reached 79.85 mg/g and 141.03 mg/g, respectively. It shows that TNs-Na has a better adsorption ability than TNs-H for Pb(II). The initial rapid adsorption probably attributed to several available active adsorption sites [37], which indicated that TNs have strong adsorption capacities for Pb(II). Then, after 20 min adsorption, the adsorption rates of TNs-H and TNs-Na for Pb(II) considerably decreased. When the adsorbing time reached 120 min, the adsorption rates remained basically invariable over time. This can be rationalized that the adsorption sites on the surface of TNs were continuously consumed, which eventually led to the saturation adsorption. Therefore, 120 min was considered to be adsorption equilibrium time of TNs.

3.2.2. Effect of initial heavy metal concentration

According to Eqs. (2) and (3), the adsorption capacities q and removal efficiency R of TNs are displayed in Fig. 5. With the increase of initial concentrations, adsorption capacities increased and eventually tended to be stable. However, the removal efficiency decreased significantly with increased initial concentrations. The plausible explanation could be a lower concentration of Pb(II) decreased the utilization of active adsorption sites, which led to a low removal efficiency. In addition, the active adsorption sites on the surface of a certain amount of TNs were limited. When the concentration of samples increased to a certain value, most of the adsorption sites occupied and adsorbed reached saturated adsorption. In other words, the redundant metal ion would not be

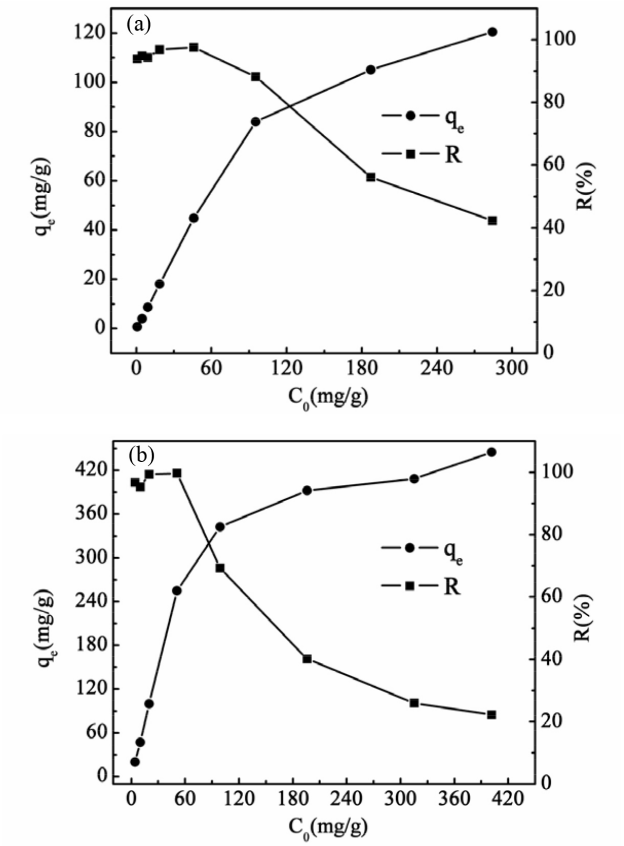

Fig. 5. Effect of initial concentration on the equilibrium adsorption capacity and removal efficiency of Pb(II) by (a) TNs-H, (b) TNs-Na.

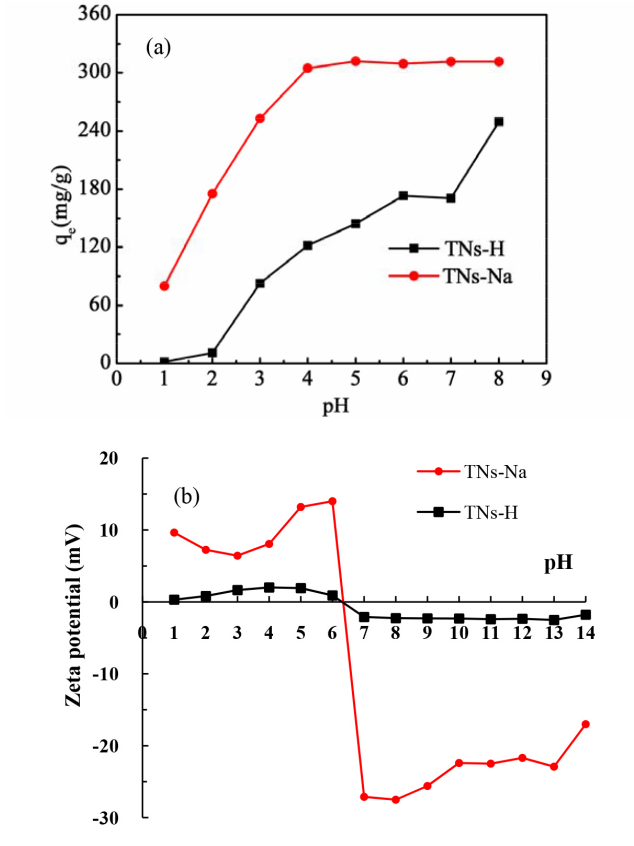

Fig. 6. (a) Effect of pH on adsorption of Pb(II) by TNs-Na and TNs-H; (b) zeta potential of TNs-Na and TNs-H.

adsorbed by TNs and then caused a decrease of the Pb(II) removal efficiency [38].

As shown in Fig. 5, the adsorption capacities of TNs for Pb(II) increased with the increasing Pb(II). When the initial concentration of Pb(II) was lower than 50 mg/L, the removal efficiencies of TNs-H and TNs-Na for Pb(II) were higher than 90%. Until the initial concentration was 200 mg/L, the adsorption capacities tended to be stable and the maximum values of adsorbed Pb(II) reached at 120 mg/g and 450 mg/g, respectively. The adsorption of Pb(II) onto TNs-Na was four times higher than that onto TNs-H. In other words, the substitution of Na^+ for H^+ after pickling led to a lower adsorption ability. It is widely accepted that mechanism of TNs adsorbing cation should be described as the exchange of cationic and Na^+ between the adjacent laminae of TNs whose exchange capacity is in proportion to the Na^+ content [22,23]. More explicit, similar behaviors were founded by Liu et al. [21] that the adsorption capacity of Cu^{2+} onto TNTs increased with an increase of Na^+ content. The adsorption capacity of TNTs, whose Na^+ content was 1.21% under pH = 5, for Cu^{2+} was 40 mg/g. By contrast, the adsorption capacity of TNTs for Cu^{2+} increased to 120 mg/g with a Na^+ content of 7.35%.

3.2.3. *Effect of pH on adsorption*

The solution pH is largely related to the surface chemistry of the adsorbent and on the chemistry of the adsorbate in solution. As shown in Fig. 6(a), the adsorption capacities of TNs-H and TNs-Na for Pb(II) was investigated by varying the pH values in the range of 1.0–8.0. Two samples had poor adsorption effect with an initial concentration of 300 mg/L at the initial pH of 1.0–2.0. Especially when the initial pH value was 1.0, the adsorption effect was considered inefficient. The equilibrium adsorption capacities of TNs-H and TNs-Na at pH = 1.0 were 1.51 mg/g and 79.80 mg/g, respectively. Thus, TNs-H is more sensitive than TNs-Na to pH value. In other words, to a certain extent, the adsorption capacity of TNs-H is pH dependent.

Furthermore, the equilibrium adsorption capacity of TNs-H increased with the increase of pH value ranged from 2.0 to 6.0, resulting from the increasing activated TNs-H surface functional groups. The Pb(II) ions may undergo hydrolysis and salvation in aqueous solution as follows [18]:

$$Pb^{2+} + nH_2O = Pb(H_2O)_n^{2+} \quad [1]$$

$$Pb(H_2O)_n^{2+} = Pb(H_2O)_{n-1}OH^+ + H^+ \quad [2]$$

$$Pb^{2+} + nH_2O = Pb(H_2O)_{n-1}OH^+ + H^+ \quad [3]$$

The adsorption capacity kept invariant and even slightly decreased from 173.42 mg/g to 170.63 mg/g as pH increased from 6.0 to 7.0, and the removal efficiency decreased from 60.98% to 60.01%. The isoelectric point of both TNs-H and TNs-Na is 6.4 from Fig. 6(b). The effect of adsorption before

and after the isoelectric point did not change much. So, the electrostatic effect did not play the main role during the adsorption. When pH increased to 8.0, the adsorption capacity and removal efficiency increased considerably to 249.80 mg/g and 87.85%, respectively. This is because the solubility product constant of Pb(II) is 1.2×10^{-15} [39], and the pH of precipitation of hydroxide is 8.2 depending on the calculations. When pH increased to 8.0, the precipitation of $Pb(OH)_2$ was formed, which led to the rapid increase in the adsorption capacity. The equilibrium adsorption capacity of TNs-Na increased with the increase of pH value ranged from 1.0 to 4.0. Adsorption amount and removal efficiency of TNs-Na increased to 304.90 mg/g and 95.88%, respectively. Thereafter, the adsorption kept stable at 310 mg/g and the removal efficiency was above 95% with an increasing pH value.

Consequently, to avoid the formation of the hydroxide precipitate, the optimum pH value of Pb(II) adsorption onto TNs-H and TNs-Na should be controlled in the ranges of 5.0–6.0 and 4.0–5.0, respectively. The results are consistent with the conclusion of Xiong et al. [34] that the optimum pH for the synthesis of titanate nanofiber was 4.0; the removal efficiency could be up to 99.8%, and the adsorption capacity increased with an increasing pH value ranged from 1.0 to 4.0. Research has found that the isoelectric point of TNTs was low ranging from 2.57 to 4.3. TNTs were positively charged when pH less than above scope, which would attract anions and repel cations electrostatically [40,41], therefore, TNTs were not easy to adsorb Pb(II) which was positively charged. Meanwhile, large numbers of H^+ in the solution competed with Pb(II) for adsorption sites, resulting in the lower adsorption capability. When pH was more than 4.3, TNTs were negatively charged, which would lead to electrostatic attraction of cations and repulsiveness of anions [40,41]. The number of negative charges increased with the increase of pH, causing binding capacities and adsorption effects of TNTs toward Pb(II) increased significantly by electrostatic attraction because TNTs had more negative charges with higher pH value.

3.2.4. Effect of titanate dosage

The adsorption capacity and removal efficiency of TNs for Pb(II) was conducted with an initial concentration of 0.1 g/L. TNs dosages in the range of 0.05–2.0 g/L were subjected to the adsorption tests. With an increasing dosage of TNs, as shown in Fig. 7, the equilibrium adsorption capacity decreased, and the removal efficiency increased. The equilibrium adsorption capacity of Pb(II) onto TNs-H and TNs-Na was 262.60 mg/g and 607.00 mg/g, respectively. While the removal efficiencies for Pb(II) reached the minimum values of 14.66% and 28.77%, respectively. The plausible explanation of the results is that the specific surface areas and the adsorption sites were limited at low TNs dosages [36]. The adsorption sites could be fully utilized at a low dosage, which further leads to the adsorption saturation and a high adsorption capacity. However, the removal efficiency of Pb(II) was low because the limited adsorption sites could not absorb a large amount of Pb(II). However, the surplus of adsorption sites would cause insufficient utilization of adsorption sites, which led to a reduced adsorption of Pb(II). For TNs-H, when dosage increased to 2.0 g/L, the equilibrium adsorption capacity decreased to the minimum value of 36.22 mg/g. While

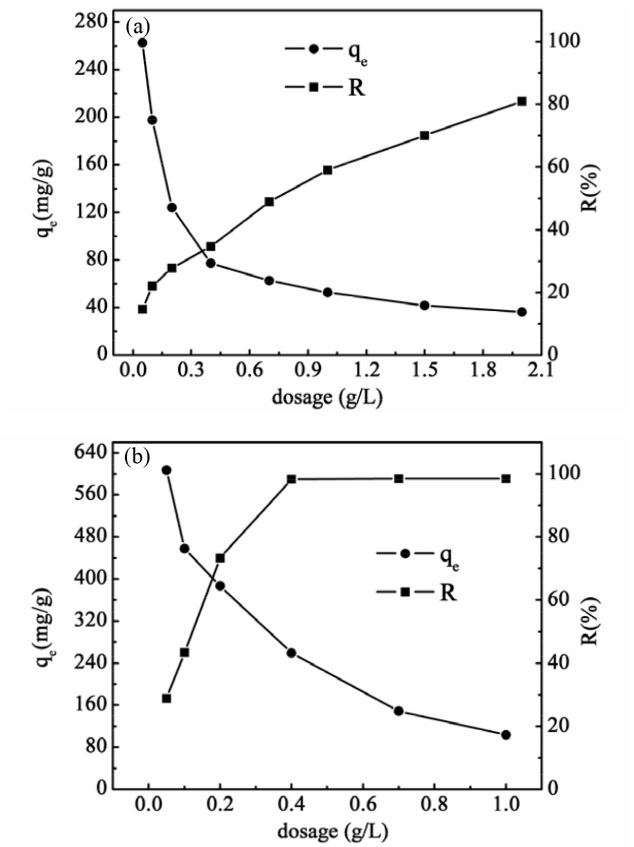

Fig. 7. Effect of adsorbent dosage on adsorption of Pb(II) by (a) TNs-H, (b) TNs-Na.

the removal efficiency increased to the maximum value of 80.88%. For TNs-Na, when dosage increased to 0.4 g/L, the equilibrium adsorption capacity decreased to 259.43 mg/g, while the removal efficiency reached 98.36%. Moreover, with an increasing TNs-Na dosage, the equilibrium adsorption capacity decreased, but the removal efficiency of heavy metal ions maintained invariable. Compared with TNs-Na, the removal efficiency of Pb(II) by TNs-H reached 80.88% only when dosage approached 2.0 g/L. The removal efficiency of Pb(II) by TNs-Na could reach 98.36% if the TNs dosage increased to 0.4 g/L. According to the result, the adsorption capacity of TNs-Na was about seven times higher than TNs-H. Therefore, to efficiently remove Pb(II) with a lower cost, TNs-Na at a lower dose was recommended to use.

3.2.5. Desorption experiments

The regeneration potential of TNs was accessed by the desorption batch experiment. As shown in Fig. 8, at pH = 1.0, the desorption rates of TNs-H and TNs-Na were 97.30% and 98.77%, respectively. This result aggresses with a similar study of Xiong et al. [34] that the desorption rate of hydrochloric acid for Pb(II) and Cd (II) from materials were 82.3% and 88.1%, respectively at pH 1.0. The desorption rate decreased with an increase of pH range from 1.0 to 3.0. There is little desorption capacity of TNs to Pb(II), the desorption rate was 0%. This result aggresses the findings of Xiong et al. [34] that the desorption rate decreased significantly with an

increasing pH value; especially when pH value was 5, the desorption rate was 0. The results showed that desorption of TNs to Pb(II) was effective, the desorption rate of TNs-H and TNs-Na all reached more than 90%.

It has been reported that the mechanism of cation desorption using acid is a competitive adsorption [42]. The competition between H^+ and cations such as Pb(II), Cu (II) and Cd (II) was strengthened by increasing the concentration of H^+. Furthermore, the hydration radius of H^+ is smaller than metal cation, which made it easier to reach the surface of TNs and had a stronger electrostatic attraction with active sites. With the accumulation of H^+ on the surface, TNs was positively charged gradually. Then the electrostatic repulsion between TNs and metal cation became stronger, which led to desorption of heavy metal.

3.2.6. Reuse of TNs-Na and TNs-H

The recycled adsorption of Pb(II) by TNs-des and TNs-re shown in Fig. 9 to find out whether TNs are suitable to reuse. It can be seen from the figure that when the initial concentration of Pb(II) was 150 mg/L and the dosage of TNs was 0.8 g/L, the adsorption capacity of TNs-Na decreased sharply during the TNs-des process and the removal rate decreased from the initial 99.98% to 4.74%. Though, TNs-H just decreased a little, from 93.22% to 92.46%.

In the process of TNs-re, the removal rate of both TNs-Na and TNs-H almost had no change, they were also more than 97% after six cycles. It showed that the regeneration of TNs can maintain a higher adsorption capacity of Pb(II). The regeneration process is essential for the recycling process of TNs. Na^+ plays the key role in the maintaining adsorption ability of TNs to Pb(II). Liu et al. [23] used the regenerated TNTs to adsorb Cd(II). They found that the molar ratio between the adsorption of Cd(II) and the amount of Na^+ by TNTs was 1:1. So, the ions of Na^+ play the key role in the TNs-Na adsorption of Pb(II).

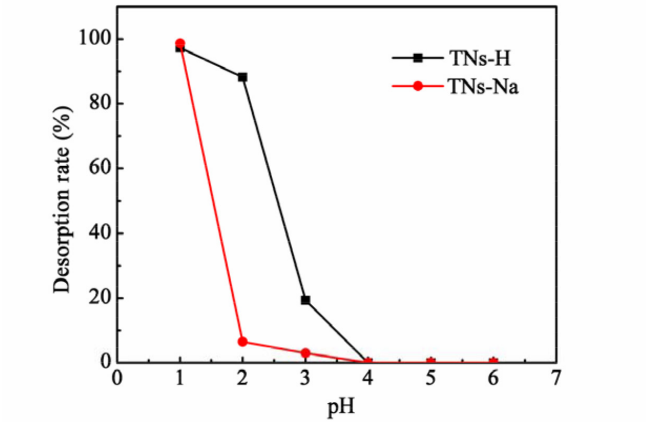

Fig. 8. Effect of pH on desorption of Pb(II) by TNs.

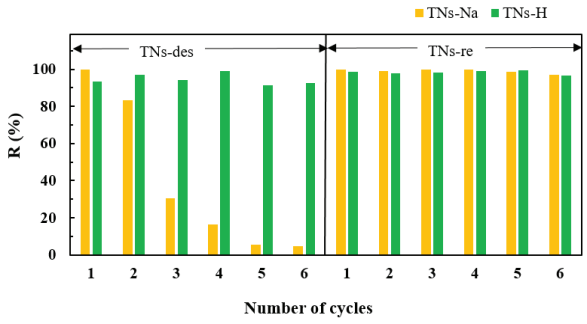

Fig. 9. Recycled adsorption of Pb(II) by TNs-des and TNs-re.

3.3. Modeling of the adsorption kinetics

The best-fit parameters of the adsorption kinetic models are shown in Table 4. Compared with the other two kinetic models, it is evident that the pseudo-second-order model provided the best fit to the experimental data. The correlation coefficient (R^2) of TNs-H and TNs-Na for Pb(II) concentrations were both 0.99. According to the kinetic models, the calculated equilibrium adsorption capacities were 85.05 and 142.34 mg/g which were consistent with the equilibrium adsorption capacity (85.59 and 142.78 mg/g) obtained from the experiment. The results indicate that the pseudo-second-order model was suitable for describing the adsorption process of Pb(II) onto TNs. Followed by pseudo-first-order kinetic model, the fitting effect of which on the adsorption of Pb(II) was also good, and the R^2 was also high, the R^2 of TNs-H and TNs-Na for Pb(II) were 0.99192 and 0.97262, respectively. In addition, the fitting effect of the intraparticle diffusion model shows the least effective with the lowest R^2 value. The R^2 values of TNs-H and TNs-Na for Pb(II) were lower than 0.35. Therefore, the particle diffusion model could not be used to descript the adsorption process of Pb(II) onto TNs. In addition, the calculated C value was high, indicating that the diffusion of particles was not the rate-limiting step. Since the pseudo-second-order model showed the best goodness of fit, chemical adsorption could be the rate-limiting step [43].

3.4. Modeling of adsorption isotherm

The curves fitted to three isotherm models of the adsorption equilibriums of Pb(II) on TNs are shown in Fig. 10. Corresponding data and fitted relation coefficient are shown in Table 5. It shows that Langmuir model provided the

Table 4
Kinetic parameters for the adsorption of Pb(II) by TNs

Kinetics models	Kinetic parameters	Materials	
		TNs-H	TNs-Na
Pseudo-first-order	q_e (mg/g)	83.09	137.77
	k_1 (1/min)	0.36	0.96
	R^2	0.99192	0.97262
Pseudo-second-order	q_e (mg/g)	85.05	142.34
	k_2 (g/(mg·min))	0.01	0.01
	R^2	0.99919	0.99915
Weber intraparticle diffusion	k_{int} (mg/(g·min$^{0.5}$))	3.29	3.56
	C (mg/g)	49.28	100.81
	R^2	0.32234	0.22669

best fit to the equilibrium adsorption data, whose correlation coefficient (R^2) of TNs-H and TNs-Na for Pb(II) were the largest of 0.99936 and 0.99912, respectively. This means that the equilibrium adsorption process followed the Langmuir model, furthermore, monolayer saturated adsorption capacity of TNs-H and TNs-Na to Pb(II) calculated by Langmuir model were 20.43 mg/g and 429.7 mg/g, respectively, which was consistent with the equilibrium adsorption capacity determined by experiment. If followed the Temkin model, the fitting effect of the adsorption to Pb(II) was also good with high R^2 that were 0.97951 and 0.96998 of TNs-H and TNs-Na, respectively. In addition, the fitting effect of Freundlich model was the least effective, the R^2 of TNs for Pb(II) was about 0.9 only.

In contrast, the q_{max} of Pb(II) on many other absorbents were compared in Table 6 [44–49]. It can be observed that TNs-Na has the highest adsorption capacity as compared with activated carbon, titanium dioxide/carbon nanotube and so on. The results exhibited the excellent adsorption ability of TNs-Na to Pb(II) and a potential application in practical.

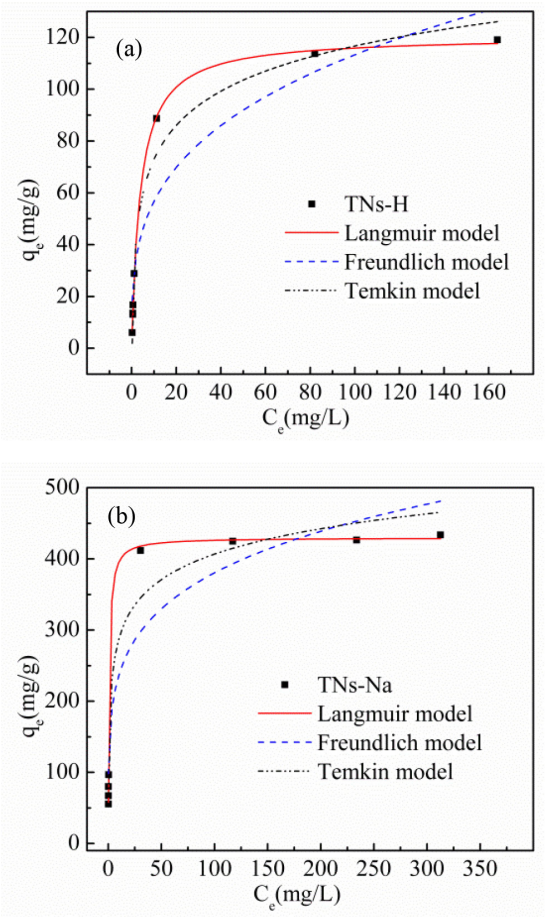

Fig. 10. Adsorption isotherm for the adsorption of Pb(II) onto TNs ((a) TNs-H, (b) TNs-Na).

3.5. Adsorption mechanism

The FT-IR spectra of TNs before and after Pb(II) adsorption were shown in Fig. 11. More explicit, before the adsorption, the main absorption peaks of TNs-H appeared at 3,192; 1,634 and 480 cm^{-1}; the main absorption peaks of TNs-Na appeared at 3,040; 1,639 and 472 cm^{-1}. According to Chen and Peng [42] and Sun and Li [50], TNTs probably had its chemical composition of titanates ($Na_xH_{2-x}Ti_3O_7$, x = 0 or 0.75, the value of x was determined by the remaining sodium ions), the basic structure of which is composed of negatively charged corrugated ribbons of edge-sharing [TiO_6] octahedra and H^+/Na^+ located between the layers, vibrational absorption of [TiO_6] octahedral mainly varied in the range from 500 to 450 cm^{-1} [50]. Then the strong adsorption bands in the region from 3,500 to 3,000 cm^{-1} and the band range from 1,630 to 1,636 cm^{-1} should be attributed to the O–H

Table 5
Isotherm parameters for the adsorption of Pb(II) onto TNs

Isotherm model	Isotherm parameters	Materials	
		TNs-H	TNs-Na
Langmuir	Q (mg/g)	120.43	429.7
	b (L/mg)	0.26	1.16
	R^2	0.99936	0.99912
Freundlich	K_F (mg/g)	28.32	147.4
	n	3.32	4.86
	R^2	0.89303	0.90155
Temkin	A (L/g)	4.62	26.55
	B (J/mol)	130.33	48.06
	R^2	0.97951	0.96998

Table 6
Comparison of maximum adsorption capacity for Pb(II) by various adsorbents

Adsorbents	Experiment conditions			q_{max} (mg/g)	Reference
	pH	T (K)	m/V (g/L)		
PAC-CNFs	5.5	301		167	[44]
Activated carbon	5	298	4	93	[45]
TiO_2/MWCNTs	6	298	2	137	[46]
Magnesium silicate hollow spheres	Solution pH value	Room temperature	0.5	300	[47]
MWCNTs	5		6.25	27.3	[48]
GO	5	298	0.1	148.7	[49]
TNs-H	5.2	273	0.2	120	This study
TNs-Na	5.2	273	0.2	450	This study

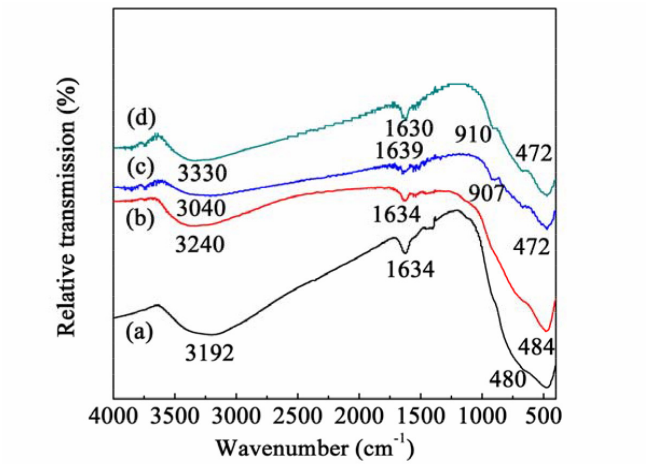

Fig. 11. FT-IR plots of (a) TNs-H, (b) TNs-H-Pb, (c) TNs-Na and (d) TNs-Na-Pb.

stretching vibration and H–O–H bending vibration, respectively, indicating the presence of hydroxyl groups and water molecules on the surface of TNTs [34,51]. The broadband at 910–900 cm^{-1} might be related to the stretching vibration of four-coordinate Ti–O including the non-bridging oxygen atom which performed in collaboration with sodium ions [50,52]. Compared with TNs-H, TNs-Na has another adsorption band at 910–900 cm^{-1}.

The FT-IR spectra of TNs-H and TNs-H which Pb(II) adsorbed on are shown in Figs. 11(b) and (d). After TNs-H adsorbing Pb(II), absorption peak at 1,634 and 480 cm^{-1} changed very little, while slight variation of absorption bands of TNs-Na at 1,639; 907 and 472 cm^{-1} was found as well, revealing that Ti–O bond, water molecules and [TiO_6] octahedron nothing to do with the adsorption of Pb(II). On the other hand, O–H stretching vibration band obtained a greater offset, absorption band of TNs-Na was significantly shifted from 3,192 to 3,240 cm^{-1} (the shift was 48 cm^{-1}) and TNs-H was significantly shifted from 3,040 to 3,330 cm^{-1} (the shift was 290 cm^{-1}), which indicated that Pb(II) had an ion exchange with hydroxyl groups of the TNs in the process of adsorption.

4. Conclusions

In conclusion, both TNs-H and TNs-Na were pure titanate of plate morphology and monoclinic phase, specific surface area of both materials were about 246 m^2/g. Compared with TNs-Na, the layer structure of TNs-H was weak, and the layer structure of TNs-H which Pb(II) adsorbed on were all damaged to some extent. The equilibrium adsorption time of two materials was 120 min. The adsorption capacity of TNs-H to Pb(II) could be up to 120 mg/g, while the adsorption capacity of TNs-Na to Pb(II) reached 450 mg/g. The adsorption kinetics of both TNs to Pb(II) followed the pseudo-second-order model and the equilibrium data were fit with the Langmuir isotherm model. The equilibrium adsorption capacity of TNs to Pb(II) increased with the pH value. The optimum pH value of adsorption of TNs-H and TNs-Na to Pb(II) should be controlled in 5.0–6.0 and 4.0–5.0, respectively. With increasing dosage of TNs, the equilibrium adsorption capacity decreased, removal efficiency increased and finally they all tended toward a steady state. When pH was 1.0, the desorption rate of TNs-H and TNs-Na was 97.30% and 98.77%, respectively. The FT-IR spectra of TNs showed that the adsorption mechanism of Pb(II) by TNs was mainly due to the ion-exchanged between Pb(II) and hydroxyl in TNs. Compared with TNs-H, the TNs-Na had stronger absorption ability and lower cost. It was found that with more sodium ions in the surface, the TNs-Na which was synthesized by water-washing had stronger absorption ability and become a kind of immense potential adsorption material for heavy metal pollution. The mechanism study showed that adsorption was mainly due to the ion-exchanged between Pb(II) and H^+/Na^+ on TNs.

Acknowledgments

The authors would like to gratefully acknowledge the financial support from the National Natural Science Foundation of China (51778146), the Outstanding Youth Fund of Fujian Province in China (No. 2018J06013), China Postdoctoral Science Foundation (2014M561856), and the Open test fund for valuable instruments and equipment of Fuzhou University (No. 2018T033). Jin Zhang would like to further acknowledge the financial support from COLABIS project (Collaborative Early Warning Information Systems for Urban Infrastructures, Grant No.: 03G0852A) funded by German Federal Ministry of Education and Research (BMBF). Mention of trade names or commercial products does not constitute endorsement or recommendation for use.

References

[1] W.S.W. Ngah, M.A.K.M. Hanafiah, Removal of heavy metal ions from wastewater by chemically modified plant wastes as adsorbents: a review, Bioresour. Technol., 99 (2008) 3935–3948.
[2] M. Hua, S. Zhang, B. Pan, W. Zhang, L. Lv, Q. Zhang, Heavy metal removal from water/wastewater by nanosized metal oxides: a review, J. Hazard. Mater., 211–212 (2012) 317–331.
[3] Z. Liab, Z. Maa, T.J.v.d. Kuijpa, Z. Yuan, L. Huang, A review of soil heavy metal pollution from mines in China: pollution and health risk assessment, Sci. Total Environ., 468–469 (2014) 843–853.
[4] Y. Su, X. Sun, X. Zhou, C. Dai, Y. Zhang, Zero-valent iron doped carbons readily developed from sewage sludge for lead removal from aqueous solution, J. Environ. Sci. China, 36 (2015) 1–8.
[5] Q. Chen, Z. Luo, C. Hills, G. Xue, M. Tyrer, Precipitation of heavy metals from wastewater using simulated flue gas: sequent additions of fly ash, lime and carbon dioxide, Water Res., 43 (2009) 2605–2614.
[6] A.G. El Samrani, B.S. Lartiges, F. Villiéras, Chemical coagulation of combined sewer overflow: heavy metal removal and treatment optimization, Water Res., 42 (2008) 951–960.
[7] R.K. Misra, S.K. Jain, P.K. Khatri, Iminodiacetic acid functionalized cation exchange resin for adsorptive removal of Cr(VI), Cd(II), Ni(II) and Pb(II) from their aqueous solutions, J. Hazard. Mater., 185 (2011) 1508–1512.
[8] M. Min, L. Shen, G. Hong, M. Zhu, Y. Zhang, X. Wang, Y. Chen, B.S. Hsiao, Micro-nano structure poly(ether sulfones)/poly(ethyleneimine) nanofibrous affinity membranes for adsorption of anionic dyes and heavy metal ions in aqueous solution, Chem. Eng. J., 197 (2012) 88–100.
[9] B.C. Ahmed, N.S. Bhadrinarayana, N. Anantharaman, M.S.B. Km, Heavy metal removal from copper smelting effluent using electrochemical cylindrical flow reactor, J. Hazard. Mater., 152 (2008) 71–78.

[10] Y. Zhang, Y. Su, X. Zhou, C. Dai, A.A. Keller, A new insight on the core–shell structure of zerovalent iron nanoparticles and its application for Pb(II) sequestration, J. Hazard. Mater., 263 (2013) 685–693.
[11] S. Yu, X. Wang, H. Pang, R. Zhang, W. Song, D. Fu, T. Hayat, X. Wang, S. Yu, X. Wang, Boron nitride-based materials for the removal of pollutants from aqueous solutions: a review, Chem. Eng. J., 333 (2018) 343–360.
[12] L. Semerjian, Equilibrium and kinetics of cadmium adsorption from aqueous solutions using untreated *Pinus halepensis* sawdust, J. Hazard. Mater., 173 (2010) 236–242.
[13] L.Y. Wang, L.Q. Yang, Y.F. Li, Y. Zhang, X.J. Ma, Z.F. Ye, Study on adsorption mechanism of Pb(II) and Cu(II) in aqueous solution using PS-EDTA resin, Chem. Eng. J., 163 (2010) 364–372.
[14] J. Li, X. Wang, G. Zhao, C. Chen, Z. Chai, A. Alsaedi, T. Hayat, X. Wang, Metal-organic framework-based materials: superior adsorbents for the capture of toxic and radioactive metal ions, Chem. Soc. Rev., 47 (2018) 2322–2356.
[15] Z. Hong, X. Zheng, X. Ding, L. Jiang, M. Wei, Complex spinel titanate nanowires for a high rate lithium-ion battery, Energy Environ. Sci., 4 (2011) 1866–1891.
[16] Z. Hong, M. Wei, Layered titanate nanostructures and their derivatives as negative electrode materials for lithium-ion batteries, J. Mater. Chem. A, 1 (2013) 4403–4414.
[17] S. Hua, X. Yu, F. Li, J. Duan, H. Ji, W. Liu, Hydrogen titanate nanosheets with both adsorptive and photocatalytic properties used for organic dyes removal, Colloids Surf., A, 516 (2017) 211–218.
[18] T.K. Naiya, A.K. Bhattacharya, S. Mandal, S.K. Das, The sorption of lead(II) ions on rice husk ash, J. Hazard. Mater., 163 (2009) 1254–1264.
[19] H. Zhang, X.P. Gao, G.R. Li, T.Y. Yan, H.Y. Zhu, Electrochemical lithium storage of sodium titanate nanotubes and nanorods, Electrochim. Acta, 53 (2008) 7061–7068.
[20] J. Huang, Y. Cao, Z. Liu, Z. Deng, W. Wang, Application of titanate nanoflowers for dye removal: a comparative study with titanate nanotubes and nanowires, Chem. Eng. J., 191 (2012) 38–44.
[21] S. Liu, C. Lee, H. Chen, C. Wang, L. Juang, Application of titanate nanotubes for Cu(II) ions adsorptive removal from aqueous solution, Chem. Eng. J., 147 (2009) 188–193.
[22] W. Liu, T. Wang, A.G.L. Borthwick, Y. Wang, X. Yin, X. Li, J. Ni, Adsorption of Pb^{2+}, Cd^{2+}, Cu^{2+} and Cr^{3+} onto titanate nanotubes: competition and effect of inorganic ions, Sci. Total Environ., 456–457 (2013) 171–180.
[23] W. Liu, H. Chen, A.G.L. Borthwick, Y. Han, J. Ni, Mutual promotion mechanism for adsorption of coexisting Cr(III) and Cr(VI) onto titanate nanotubes, Chem. Eng. J., 232 (2013) 228–236.
[24] M. Wei, Y. Konishi, H. Arakawa, Synthesis and characterization of nanosheet-shaped titanium dioxide, J. Mater. Sci., 42 (2007) 529–533.
[25] K.W. Kolasniski, Zur theorie der sogenannten adsorption gelöster stoffe, K. Sven. Vetensk.akad., 179 (2001) 118–119.
[26] G. Blanchard, M. Maunaye, G. Martin, Removal of heavy metals from waters by means of natural zeolites, Water Res., 18 (1984) 1501–1507.
[27] I. Langmuir, The constitution and fundamental properties of solids and liquids. Part i. solids, J. Franklin I, 184 (1916) 102–105.
[28] H.M.F. Freundlich, Over the adsorption in solution, J. Phys. Chem. A, 57 (1906) 1100–1107.
[29] T.M. J, P. V, Recent modifications to Langmuir isotherms, Acta Physicochim, URSS, 12 (1940) 217–222.
[30] I. Langmuir, The adsorption of gases on plane surfaces of glass, mica and platinum, J. Am. Chem. Soc., 40 (1918) 1361–1403.
[31] H.M.F. Freundlich, Over the adsorption in solution, Phys. Chem, 57 (1906) 385-470.
[32] D.L. Morgan, H. Liu, R.L. Frost, E.R. Waclawik, Implications of precursor chemistry on the alkaline hydrothermal synthesis of titania/titanate nanostructures, J. Phys. Chem. C, 114 (2010) 101–110.
[33] C. Lee, K. Lin, C. Wu, M. Lyu, C. Lo, Effects of synthesis temperature on the microstructures and basic dyes adsorption of titanate nanotubes, J. Hazard. Mater., 150 (2008) 494–503.
[34] L. Xiong, C. Chen, Q. Chen, J. Ni, Adsorption of Pb(II) and Cd(II) from aqueous solutions using titanate nanotubes prepared via hydrothermal method, J. Hazard. Mater., 189 (2011) 741–748.
[35] T. Wang, W. Liu, N. Xu, J. Ni, Adsorption and desorption of Cd(II) onto titanate nanotubes and efficient regeneration of tubular structures, J. Hazard. Mater., 250–251 (2013) 379–386.
[36] J. Huang, Y. Cao, Q. Huang, H. He, Y. Liu, High-temperature formation of titanate nanotubes and the transformation mechanism of nanotubes into nanowires, Cryst. Growth Des., 9 (2009) 911–912.
[37] A.R. Iftikhar, H.N. Bhatti, M.A. Hanif, R. Nadeem, Kinetic and thermodynamic aspects of Cu(II) and Cr(III) removal from aqueous solutions using rose waste biomass, J. Hazard. Mater., 161 (2009) 941–947.
[38] M. Rafatullah, O. Sulaiman, R. Hashim, A. Ahmad, Adsorption of copper (II), chromium (III), nickel (II) and lead (II) ions from aqueous solutions by meranti sawdust, J. Hazard. Mater., 170 (2009) 969–977.
[39] A. Saeed, M. Iqbal, M.W. Akhtar, Removal and recovery of lead(II) from single and multimetal (Cd, Cu, Ni, Zn) solutions by crop milling waste (black gram husk), J. Hazard. Mater., 117 (2005) 65–73.
[40] H. Niu, Y. Cai, Preparation of octadecyl and amino mixed group modified titanate nanotubes and its efficient adsorption to several ionic or ionizable organic analytes, Anal. Chem., 81 (2009) 9913–9920.
[41] H.Y. Niu, J.M. Wang, Y.L. Shi, Y.Q. Cai, F.S. Wei, Adsorption behavior of arsenic onto protonated titanate nanotubes prepared via hydrothermal method, Microporous Mesoporous Mater., 122 (2009) 28–35.
[42] Q. Chen, L. Peng, Structure and applications of titanate and related nanostructures, Int. J. Nanotechnol., 4 (2007) 261–270.
[43] Y.S. Ho, G. Mckay, Sorption of dye from aqueous solution by peat, Chem. Eng. J., 70 (1998) 115–124.
[44] A. Al Mamun, Y.M. Ahmed, M.a.F.R. AlKhatib, A.T. Jameel, M.A.H.A.R. AlSaadi, Lead sorption by carbon nanofibers grown on powdered activated carbon—kinetics and equilibrium, Nano, 10 (2015) 1550017.
[45] A. Kongsuwan, P. Patnukao, P. Pavasant, Binary component sorption of Cu(II) and Pb(II) with activated carbon from *Eucalyptus camaldulensis Dehn* bark, J. Ind. Eng. Chem., 15 (2009) 465–470.
[46] X. Zhao, Q. Jia, N. Song, W. Zhou, Y. Li, Adsorption of Pb(II) from an aqueous solution by titanium dioxide/carbon nanotube nanocomposites: kinetics, thermodynamics, and isotherms, J. Chem. Eng. Data, 55 (2010) 4428–4433.
[47] Y. Wang, G. Wang, H. Wang, C. Liang, W. Cai, L. Zhang, Chemical-template synthesis of micro/nanoscale magnesium silicate hollow spheres for waste-water treatment, Chemistry (Weinheim an der Bergstrasse, Germany), 16 (2010) 3497–3503.
[48] X.L. Tian, Z. Shan, Z.Y. Zhang, H. Xiao, M.J. Yu, D.H. Lin, Metal impurities dominate the sorption of a commercially available carbon nanotube for Pb(II) from water, Environ. Sci. Technol., 44 (2010) 8144.
[49] Y. Du, J. Wang, Y. Zou, W. Yao, J. Hou, L. Xia, A. Peng, A. Alsaedi, T. Hayat, X. Wang, Synthesis of molybdenum disulfide/reduced graphene oxide composites for effective removal of Pb(II) from aqueous solutions, Sci. Bull., 62 (2017) 913–922.
[50] X. Sun, Y. Li, Synthesis and characterization of ion-exchangeable titanate nanotubes, Chemistry, 9 (2003) 2229–2238.
[51] M. Qamar, C.R. Yoon, H.J. Oh, N.H. Lee, K. Park, D.H. Kim, K.S. Lee, W.J. Lee, S.J. Kim, Preparation and photocatalytic activity of nanotubes obtained from titanium dioxide, Catal. Today, 131 (2008) 3–14.
[52] Y. Chen, S. Lo, J. Kuo, Pb(II) adsorption capacity and behavior of titanate nanotubes made by microwave hydrothermal method, Colloids Surf., A, 361 (2010) 126–131.